Isobaric tags for relative and absolute quantitation-based quantitative proteomic analysis of X-linked inhibitor of apoptosis and H2AX in etoposide-induced renal cell carcinoma apoptosis

Tian-Shu Liu[1], Chao Chen[1], Biao Zhou[2], Bo-Wen Xia[1], Zong-Ping Chen[3], Yong Yan[1]

[1]Department of Urology, Beijing Shijitan Hospital, Capital Medical University, Beijing 100038, China;
[2]Department of Vascular Surgery, People's Hospital of Peking University, Beijing 100044, China;
[3]Department of Urology, The Affiliated Hospital of Zunyi Medical College, Zunyi, Guizhou 563000, China.

Abstract

Background: X-linked inhibitor of apoptosis (XIAP) is a vital factor in the anti-apoptosis mechanism of tumors and is highly expressed in renal cell carcinoma (RCC). However, the mechanism through which XIAP regulates DNA damage repair is unknown. This study investigated the regulatory mechanism of XIAP in etoposide-induced apoptosis in two Caki-1 cell lines with high or low XIAP expression.

Methods: The two cell lines were established using RNA interference technology. The differentially expressed proteins in the two cell lines were globally analyzed through an isobaric tags for relative and absolute quantitation-based quantitative proteomics approach. Proteomic analysis revealed 255, 375, 362, and 5 differentially expressed proteins after 0, 0.5, 3, and 12 h of drug stimulation, respectively, between the two cell lines. The identified differentially expressed proteins were involved in numerous biological processes. In addition, the expression of histone proteins (H1.4, H2AX, H3.1, H3.2, and H3.3) was drastically altered, and the effects of XIAP silencing were accompanied by the marked downregulation of H2AX. Protein-protein interactions were assessed and confirmed through immunofluorescence and Western blot analyses.

Results: The results suggested that XIAP may act as a vital cell signal regulator that regulates the expression of DNA repair-related proteins, such as H2AX, and influences the DNA repair process.

Conclusions: Given these functions, XIAP may be the decisive factor in determining the sensitivity of RCC cell apoptosis induction in response to chemotherapeutic agents.

Keywords: Apoptosis; H2AX; iTRAQ; Renal cell carcinoma; X-linked inhibitor of apoptosis

Introduction

Renal cell carcinoma (RCC) is one of the most common malignant urological tumors and accounts for approximately 2% of all cancer cases worldwide.[1] The 5-year survival rate of patients with metastatic RCC is less than 10% given the chemo- and radiotherapy resistance of this malignancy. RCC is highly resistant to chemotherapy because of its high apoptosis threshold. Various factors, such as overexpression of X-linked inhibitor of apoptosis (XIAP), contribute to the progression and chemo-resistance of RCC. XIAP expression is higher in RCC than in autologous normal kidneys, and XIAP overexpression in RCC is predictive of poor prognosis.[2] Our previous research showed that RCC cells with high XIAP expression are resistant to apoptosis stimulation, whereas those with low XIAP expression are sensitive to apoptotic signals. XIAP expression is unaffected by apoptosis stimulation.[3]

Among all members of the inhibitor of apoptosis (IAP) family, the caspase inhibition mechanism of XIAP is the best characterized,[4] and XIAP is the most promising target for tumor therapy. XIAP contains three BIR domains and a RING domain. The Baculovirus IAP Repeats-2 (BIR-2) domain binds and potently inhibits caspase-3 and caspase-7, and the BIR3 domain and the flanking regions suppress caspase-9.[5] The RING domain of XIAP exhibits E3 ubiquitin ligase activity and labels target proteins with ubiquitin molecules, thereby promoting protein degradation through ubiquitination.[6] Recent technological advancements have furthered our current understanding of the function of XIAP. In addition to inhibiting caspase activity, XIAP inhibits apoptosis by participating in other

Access this article online

Quick Response Code:

Website: www.cmj.org

DOI: 10.1097/CM9.0000000000000553

Correspondence to: Yong Yan, Department of Urology, Beijing Shijitan Hospital, Haidian District, 10 Iron Medical Road, Beijing 100038, China
E-Mail: yanyongsjt@163.com

Chinese Medical Journal 2019;132(24)

Received: 17-07-2019 **Edited by:** Xiu-Yuan Hao

signal transduction pathways. Specifically, XIAP inhibits cell apoptosis by binding of the RING domain to the BMP receptor to influence the TGF-Beta Activated Kinase 1 Binding Protein 1 (TAB1)-TGF-Beta-Activated Kinase 1 (TAK1)-Jun Proto-Oncogene 1 (JNK1) signal transduction pathway.[7] The Mitogen-Activated Protein Kinase 1 (MEK1) and phosphatidylinositol 3-kinase (PI3K) signaling pathways may also be involved in the apoptosis inhibition mediated by XIAP.[8] Moreover, XIAP participates in mammary development and T-cell maturation.[9] XIAP performs other biological functions aside from inhibiting caspases. These functions are generally related to specific domains of XIAP. Upon drug-induced apoptosis in lymphoma cells, XIAP is translocated from the cytosol to the nucleus.[10] However, the role of XIAP in the nucleus remains unclear, and existing studies have primarily focused on the regulation of XIAP in the cytoplasm. Furthermore, RCC cells are resistant to radiation-induced apoptosis, which can cause DNA damage in the nucleus.[11] Thus, the present study focused on the effect of nuclear XIAP on apoptosis induced by DNA damage.

Whether tumor cells initiate DNA repair or apoptosis depends on the extent of DNA damage, and the histone variant H2AX plays an important role in this process. Upon DNA damage, PI3K family members ataxia telangiectasia-mutated gene (ATM), ATM and Rad-3 ralated (ATR), and DNA-dependent protein kinase (DNA-PK) phosphorylate H2AX on Ser139 to generate γ-H2AX.[12] The phosphorylated form of H2AX can facilitate anchoring of signaling and repair proteins, such as Meiotic recombination 11 homolog A (MRE11), Double strand break repair protein (RAD50), MRN complex (Nijmegen Breakage Syndrome 1 [NBS1]/MRE11/RAD50), and Mediator of DNA Damage Checkpoint 1 (NFBD1)/DNA damage checkpoint 1 (MDC1), to form γ-H2AX foci at sites of DNA double-strand breaks.[13] The phosphorylation of tyrosine 142 in H2AX prevents recruitment of the repair complex and promotes binding of pre-apoptotic factors, such as JNK1, thereby directly promoting cell apoptosis.[14,15] Although these findings suggest that XIAP and H2AX play important roles in apoptosis, no study has explored the interaction between these two proteins.

Etoposide is a topoisomerase II inhibitor that is used to treat a broad spectrum of human cancers. It can induce cells to produce DNA strand breaks and promote tumor apoptosis in a dose-dependent manner.[16] In this study, we combined RNA interference (RNAi) technology with an isobaric tags for relative and absolute quantitation (iTRAQ)-based quantitative proteomics approach to globally profile the function of XIAP in etoposide-induced apoptosis of RCC cells. We stably knocked down XIAP in an RCC (Caki-1) cell line and compared the proteome of XIAP knockdown cells with that of the original Caki-1 cells following etoposide treatment. We found that XIAP is involved in numerous novel biological functions in etoposide-induced apoptosis. Our results demonstrate for the first time that XIAP regulates DNA repair mechanisms by downregulating the expression of H2AX protein. In turn, this downregulation of H2AX protein expression may prolong JNK activation and apoptosis initiation.

Methods

Cell culture and treatment

Caki-1 cells were purchased from China Infrastructure of Cell Line Resources (Beijing, China), grown in minimum essential medium (Gibco; Thermo Fisher Scientific, Inc., Waltham, MA, USA) supplemented with 10% fetal bovine serum (Zhejiang Kang Yuan Biological Technology Co., Ltd., Zhuji, China), and maintained at 37°C in a humidified incubator with 5% CO_2. At approximately 90% confluence, the cells were washed with phosphate-buffered saline and then treated with 60 μg/mL etoposide (Aldrich, Sigma, St. Louis, MO 63178, USA) or with serum-free medium as a control. The concentration of etoposide was based on our previous experimental data.[17]

RNAi

At 70% confluence, Caki-1 cells were transfected with either XIAP small interfering RNA or control short hairpin RNA (shRNA) using Lipofectamine 2000 in accordance with the manufacturer's instructions (Invitrogen, USA). XIAP expression after transfection was assessed through immunoblotting. The XIAP interference target was based on that described in a study by Bilim *et al*,[18] who verified the absence of homologous sequences between this fragment and other genes and showed that XIAP expression is downregulated by shRNA that contains this fragment. The target sequence was 5′-AGGTGAAGGTGATAAAGTA-3′. A BLOCK-iT™ U6 RNAi Entry Vector kit (Invitrogen; Thermo Fisher Scientific, Inc.) was adopted for construction. On the basis of the selected target sequence, the following shRNA oligonucleotide sequences were used: 5′-CACC-GAGGTGAAGGTGATAAAGTACGAATACTTTATCA CCTTCACC-3′ (top strand) and 5′-AAAAGGTGAAGGT-GATAAAGTATTCGTACTTTATCACCTTCACCTC-3′ (bottom strand). At 48 h post-transfection, the medium was replaced with fresh selection medium containing geneticin (Kang Wei Technology, Beijing, China) to screen for stably transfected cells. Culture medium was replaced with fresh selection medium every 2 days until no cells were killed.

Cell lysate preparation and Western blot analysis

Total protein was extracted at different time points after etoposide induction. Protein concentration was determined using a bicinchoninic acid protein assay kit. Whole cell lysates were prepared using Radio Immunoprecipitation Assay (RIPA) reagent (Bioeasytech, China). A total of 40 μg of protein from each sample was resolved through sodium dodecyl sulfate (SDS)-polyacrylamide gel electrophoresis and transferred to polyvinylidene fluoride membranes. The membranes were blocked overnight with 5% non-fat milk and probed with primary antibodies against target proteins at 4°C overnight, followed by incubation with secondary anti-rabbit (1:10,000 dilution; Bioeasytech) or anti-mouse (1:20,000 dilution; Bioeasytech) antibody at 37°C for 45 min. The antibodies used in this study (targeting XIAP [1:500], β-Actin [1:2000], H2AX [1:500], and glyceraldehyde 3-phosphate dehydrogenase [1:400]) were purchased from Cell Signaling Technology. The relative intensity of each band was digitized using BandScan V4.3.

iTRAQ analysis

XIAP knockdown and original Caki-1 cells were treated with 60 μg/mL etoposide for 0.5, 3, and 12 h. Exactly 2 mL of lysis buffer (8 mol/L urea, 30 mmol/L N-2-hydroxyethylpiperazine-N'-2-ethanesulfonic acid, 1 mmol/L phenylmethylsulfonyl fluoride, 2 mmol/L ethylenediaminetetraacetic acid, and 10 mmol/L dithiothreitol) was added to each sample. Each sample was then sonicated on ice and centrifuged at 13,000 r/min for 10 min at 4°C. Proteins were precipitated with ice-cold acetone before redissolution in dissolution buffer (50% triethylamonium bicarbonat and 0.1% SDS). Proteins were quantified through a Bradford protein assay (Promega Corporation, Madison, WI, USA). Subsequently, 100 mg of protein was digested with trypsin, and the resultant peptide mixture was labeled using the appropriate iTRAQ reagents (Applied Biosystems; Thermo Fisher Scientific, Inc.) dissolved in 70 μL of isopropanol. Protein samples were labeled with the iTRAQ isobaric tags 113, 114, 115, 116, 117, 118, 119, and 121.

To reduce sample complexity during liquid chromatography tandem mass spectrometry (LC-MS/MS) analysis (strong cation exchange chromatography [SCX]), iTRAQ-labeled peptide samples were reconstituted in Buffer A (25% acetonitrile [ACN], 10 mmol/L KH_2PO_4; pH 3.0) and fractionated using an Ultremex SCX column (Phenomenex, Torrance, CA, USA; Luna SCX 100A) via an LC-20AB HPLC pump system (Shimadzu Corporation, Kyoto, Japan) at a flow rate of 1.0 mL/min with a gradient of Buffer B (25% ACN, 2 mol/L KCL, 10 mmol/L KH_2PO_4; pH 3.0). Buffer B reached 100% within 10 min. The column flow rate was maintained at 400 nL/min, and the column temperature was maintained at room temperature under a pressure of 1000 psi. The collected fractions were desalted using a Strata X C18 column (Phenomenex), vacuum centrifuged (4°C and 20,000 × *g* for 30 min), and reconstituted in 0.1% formic acid for subsequent LC-MS/MS analysis. Mass spectroscopy (MS) analysis was performed using a Q Exactive™ Hybrid Quadrupole-Orbitrap™ Mass Spectrometer (Thermo Fisher Scientific, Inc.). The peptide samples were subjected to nanoflow electrospray ionization MS/MS analysis on an Eksigent NanoLC-2D system (AB SCIEX, Framingham, MA, USA).

MS and MS/MS data searches were performed using Proteome Discoverer 1.3 (Thermo Fisher Scientific, Inc.) on the basis of the workflow with a spectrum selector and a reporter ion quantifier. Proteins were identified and quantified using the Mascot search engine (version 2.3.0; Matrix Science Inc., Boston, MA, USA). Peptides were automatically selected for iTRAQ quantification by the progroup algorithm (at least two peptides with 99% confidence). The reporter peak area, error factor, and *P* value were calculated. Proteins had to contain at least two unique high-scoring peptides for selection as a differentially expressed protein.

Double-labeling immunofluorescence

Caki-1 cells and XIAP knockdown cells were incubated with specific primary antibodies against XIAP (1:100; Cell Signaling Technology) and H2AX (1:100; Abcam Inc., Cambridge, MA, USA). As previously described, the cells were subsequently incubated for 1 h at 21°C with Alexa Fluor® 594-goat anti-rabbit or Alexa Fluor® 488-goat anti-mouse secondary antibody and with 4′,6-diamino-2-phenylindole (DAPI) for nuclear staining.[19] Immunofluorescence was visualized using a confocal fluorescence microscope (Nikon A1R/A1) under 600× magnification. Fluorescence was quantified using ImageJ software, and at least 50 nuclei were analyzed.

Statistical analysis

SPSS 17 (SPSS Inc., IBM, Chicago, IL, USA) software was used for statistical analysis. The data were subjected to analysis of variance, and means were compared through Duncan multiple-range test. $P < 0.05$ was considered statistically significant.

Results

Stable knockdown of XIAP by shRNA in sensitized Caki-1 cells to etoposide

To investigate the role of XIAP in etoposide-induced apoptosis of RCC cells, we knocked down XIAP expression in Caki-1 cell lines through RNAi technology. We confirmed the interference efficiency in XIAP knockdown cells through Western blot analysis. As shown in Figure 1, XIAP expression decreased in cells transfected with XIAP shRNA relative to that in cells transfected with the control shRNA and in the original cells. To examine the effect of XIAP on apoptosis of Caki-1 cells, we used Annexin V-fluorescein (FITC)/propidium iodide (PI) Apoptosis Detection Kits to assess the apoptosis rates of XIAP knockdown cells and original Caki-1 cells. The flow cytometry results indicated that after 24 h of etoposide treatment, the total apoptosis rate of the XIAP knockdown cells was 4.2-fold higher than that of the original Caki-1 cells [Figure 2].

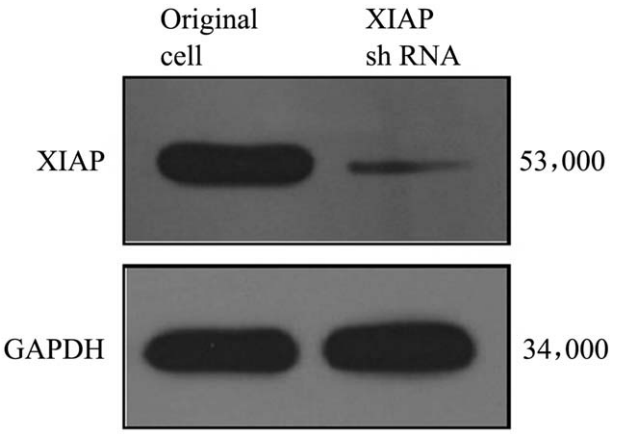

Figure 1: Confirmation of XIAP knockdown efficiency. Validation of XIAP expression in knockdown cells (XIAP shRNA) and original Caki-1 cells through Western blot analysis. GAPDH expression was used as a loading control. GAPDH: Glyceraldehyde 3-phosphate dehydrogenase; shRNA: Short hairpin RNA; XIAP: X-linked inhibitor of apoptosis.

Numerous differentially expressed proteins were identified through iTRAQ profiling

To investigate the global effect of XIAP on etoposide-induced apoptosis, we subjected the original Caki-1 and XIAP knockdown cells to iTRAQ-based quantitative proteomics analysis. Cells were treated with 60 μg/mL etoposide for 0, 0.5, 3, or 12 h. We used iTRAQ 117, 118, 119, and 121 tags to label the knockdown XIAP cells at these four-time points. We used iTRAQ 113, 114, 115, and 116 tags to label the original Caki-1 cells.

We identified 1783 non-redundant differentially expressed proteins in the two cell lines. For the subsequent relative quantification analysis, although statistical analysis is part of the ProteinPilot software, we applied an additional ≥1.3 or ≤0.77 (1/1.3)-fold cut-off to all iTRAQ ratios to minimize false positives when proteins were identified as over- or underexpressed. We adopted this cut-off value because the overall technical variation in the data from duplicate experiments was estimated to be less than 30% and because this value has been widely used in other investigations that used the iTRAQ approach.[20] Proteins with iTRAQ ratios below 0.77 were considered underexpressed, whereas those with ratios greater than 1.3 were considered overexpressed.

By applying this filter, we identified 255, 375, 362, and 5 significantly altered proteins in Caki-1 and XIAP knockdown cells at 0, 0.5, 3, and 12 h, respectively. Then, we conducted gene ontology (GO) enrichment analysis to better understand the molecular and functional characteristics of these differentially expressed proteins. Figure 3A–C shows the distribution of differentially expressed proteins in cellular component, biological processes, and molecular functions at 0.5 h of etoposide treatment. A total of 3521 biological processes, 577 protein classes, and 710 molecular functions were classified. At the same time,

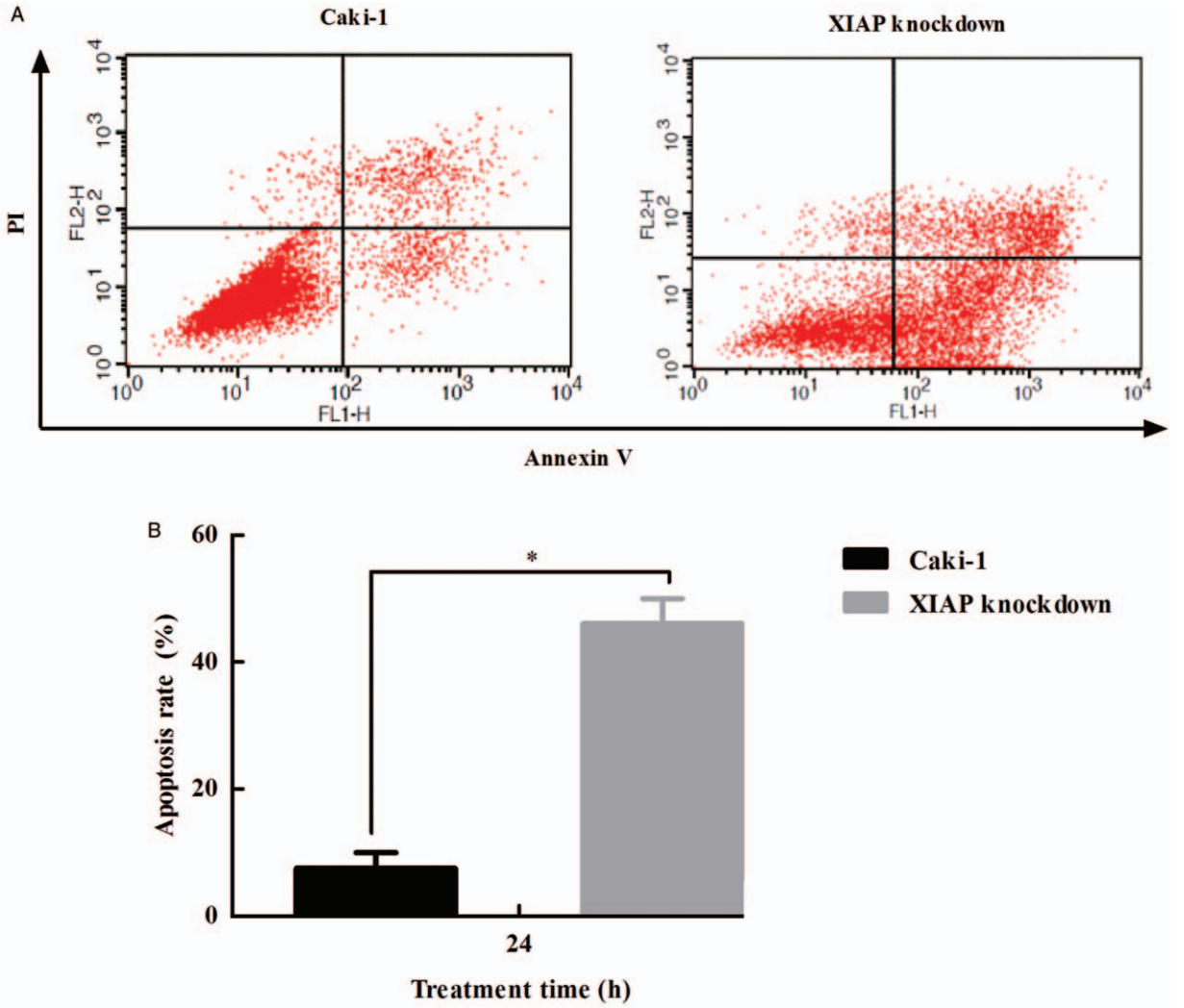

Figure 2: Examination of cell apoptosis through Annexin V-FITC and propidium iodide staining followed by flow cytometry. (A) Representative flow cytometry results from repeated experiments. Cells were characterized as early apoptotic (bottom right quadrant), late apoptotic (top right quadrant) or healthy cells (bottom left quadrant) on the basis of flow cytometry results. The total apoptosis rates (B) are summarized in a bar chart. The values are expressed as the mean ± SD of three independent experiments; $^{*}P < 0.001$. SD: Standard deviation; XIAP: X-linked inhibitor of apoptosis.

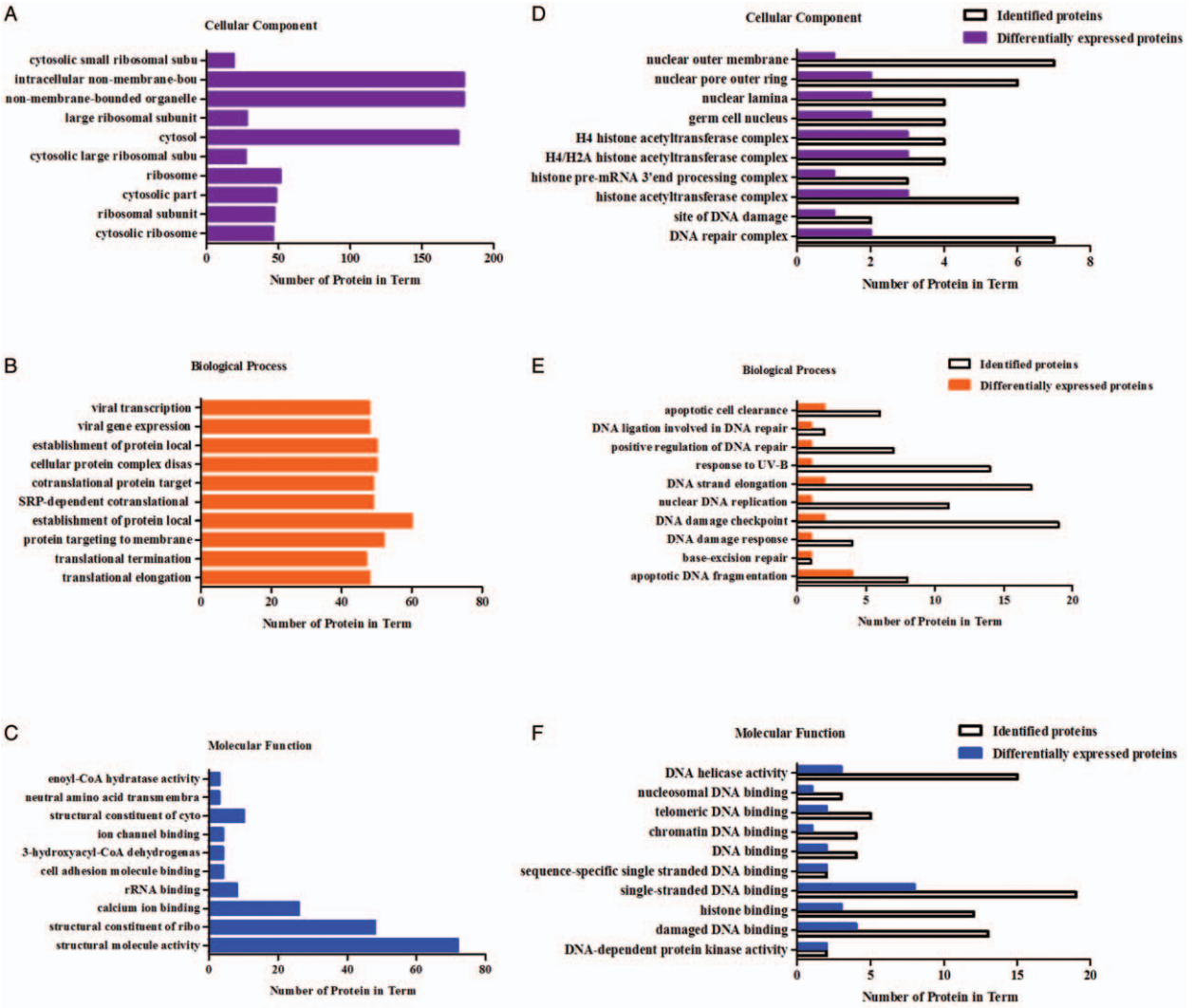

Figure 3: Results of GO enrichment analysis (at 0.5 h as an example) Differentially expressed proteins were identified as participants in (A) cellular component, (B) biological process, or (C) molecular function. The figure presents the pathway analysis results and shows the distribution of the differentially expressed proteins (Fisher exact test, $P < 0.05$) in each classification; the top ten results were selected after sorting on the basis of *P* value. (D–F) represent the classifications related to the nucleus, histone, DNA damage, and DNA repair and include the identified non-redundant proteins and differentially expressed proteins. GO: Gene ontology.

many classifications related to the nucleus and DNA were found, such as DNA repair complex, damaged DNA binding, and DNA damage checkpoint. All these classifications included numerous differentially expressed proteins. Functional annotations were obtained from the GO database (http://www.geneontology.org/).

XIAP knockdown changed the expression of many histone variants during etoposide-induced apoptosis

Etoposide can cause DNA double-strand breaks. Histone modifications can serve as damage markers and play a crucial role in DNA repair.[21] GO analysis revealed numerous differentially expressed proteins that participate in various nuclear-related cellular components, including the nucleus, DNA damage, and DNA repair. Thus, we studied changes in histones in the two cell lines. We identified 14 histone protein variants. By using the above criteria ($P < 0.05$, iTRAQ ratio ≥ 1.3 or ≤ 0.77), we found that at 12 h after stimulation of apoptosis, the number of differentially expressed proteins between the two cell lines drastically decreased. Table 1 shows that the expression levels of five proteins (H1.4, H2AX, H3.1, H3.2, and H3.3) at three-time points (0, 0.5, and 3 h) were significantly altered by etoposide treatment and that only H2AX was downregulated at 0 h. The ratios of 113:117, 114:118, 115:119, and 116:121 indicate the relative abundance levels of H2AX protein [Figure 4] in Caki-1 cells compared with those in the XIAP knockdown group at four different time points after etoposide treatment.

The H2AX expression trend detected through Western blot analysis was consistent with that detected through iTRAQ analysis

The phosphorylation status of the histone variant H2AX S139 changes after DNA damage. Thus, H2AX was selected for further validation on the basis of its highly

Table 1: Identified non-redundant histone proteins.

Accession	Description	Different times ratio (Caki-1/XIAP knockdown)			
		0 h	0.5 h	3 h	12 h
P10412	Histone H1.4 GN=HIST1H1E [H14_HUMAN]	1.53	0.63	0.66	1.15
P16104	Histone H2AX GN=H2AFX[H2AX_HUMAN]	0.77	0.31	0.38	0.99
P68431	Histone H3.1 GN=HIST1H3A [H31_HUMAN]	1.91	0.29	0.32	0.69
Q71DI3	Histone H3.2 GN=HIST2H3A [H32_HUMAN]	1.35	0.22	0.28	0.88
P84243	Histone H3.3 GN=H3F3A [H33_HUMAN]	1.52	0.26	0.39	0.84

XIAP: X-linked inhibitor of apoptosis.

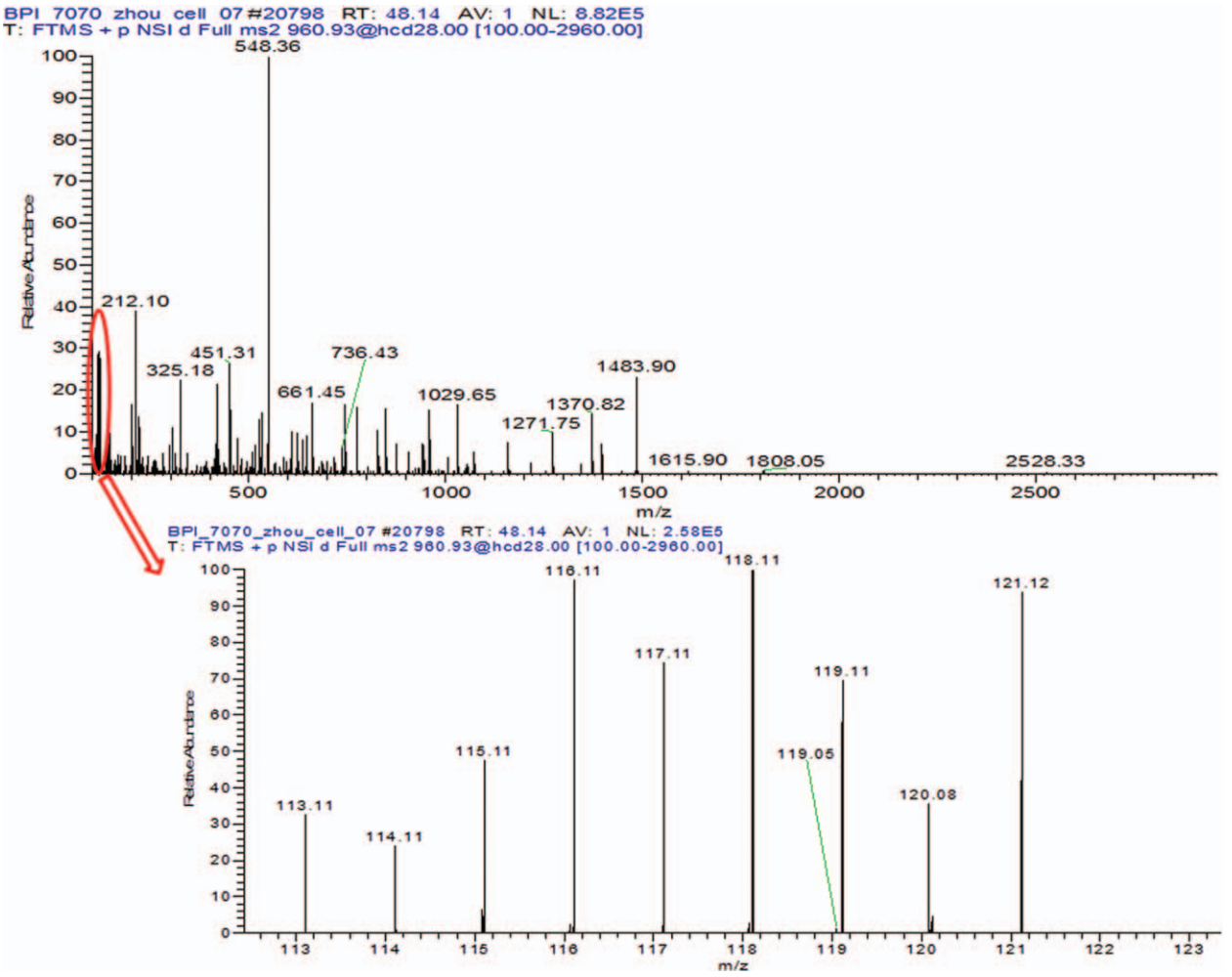

Figure 4: Relative abundance of H2AX.

significant ratios and its relevance to apoptosis. Western blot analysis results for H2AX expression in the two cell lines are shown in Figure 5. H2AX was downregulated in Caki-1 cells but not in XIAP knockdown cells. Although this change in expression detected through immunoblot analysis was consistent with that detected through iTRAQ, some differences were detected between the two techniques. These differences could be attributed to various factors, such as antibody potency, differences inherent to each technical approach, and other uncertainties. Nevertheless, both techniques consistently showed that H2AX expression was significantly downregulated in Caki-1 cells compared with XIAP knockdown cells.

Cellular distribution of XIAP and H2AX

We used double immunofluorescence labeling to investigate the sub-cellular distribution of H2AX and its potential interaction with XIAP. We subjected Caki-1 cells and XIAP knockdown cells to XIAP-specific immunofluores-

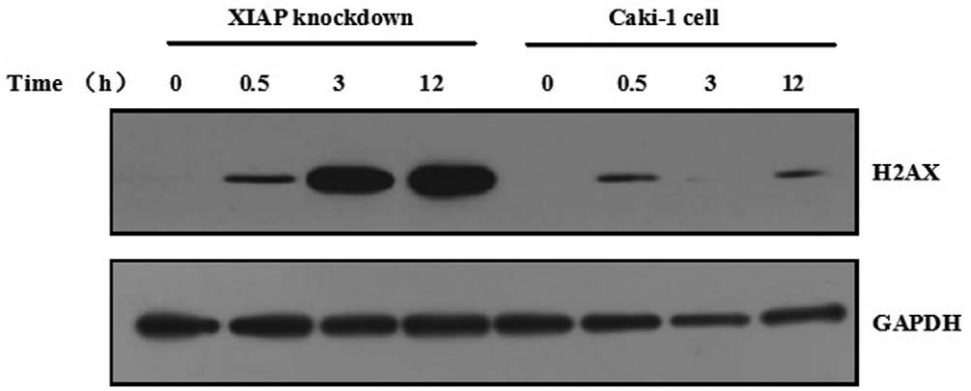

Figure 5: Validation of iTRAQ data through Western blot analysis. H2AX was selected for validation of the expression alteration trends through Western blot analysis. The results showed that H2AX is downregulated in Caki-1 cells compared with XIAP knockdown cells after etoposide treatment. GAPDH was used as a loading control. GAPDH: Glyceraldehyde 3-phosphate dehydrogenase; XIAP: X-linked inhibitor of apoptosis.

cence (XIAP-IF) and H2AX-specific immunofluorescence (H2AX-IF) analyses. We performed nuclear staining with DAPI, a dye that binds to nucleic acids and stains cell nuclei. Confocal microscopy (100×) showed that XIAP-IF was primarily localized in cellular cytosolic protein aggregates and in the perinuclear region of the cytoplasm of Caki-1 cells [Figure 6A]. However, we found that immunofluorescence corresponding to H2AX protein (green) was mostly localized in the nucleus. Merged images revealed that XIAP (red) and H2AX (green) did not colocalize in the nucleus or cytoplasm of Caki-1 cells. Areas of XIAP and H2AX colocalization would have appeared as yellow/orange fluorescence. This result shows that XIAP does not interact directly with H2AX via E3 ubiquitin ligase but may indirectly regulate H2AX through other pathways. XIAP and H2AX displayed the same distribution in the two cell lines. Moreover, consistent with the Western blot analysis and iTRAQ results, the mean fluorescence intensity of H2AX in XIAP knockdown cells was higher than that in Caki-1 cells [Figure 6B].

Discussion

RCC is a major urological cancer with increasing incidence rates and high lethality.[22] An extensive number of studies have suggested that apoptosis resistance is the primary cause of RCC therapy failure. However, the molecular mechanisms underlying the apoptosis resistance of RCC require further clarification. XIAP is an anti-apoptotic protein that suppresses cell death by potently inhibiting caspases[23] High XIAP levels in RCC models are associated with the poor clinical outcome of patients with RCC.[24] Our study assessed the effect of the XIAP level on the sensitivity of RCC cells to apoptosis.

XIAP, one of the most important IAPs, is characterized by the presence of a RING finger that confers E3 ubiquitin ligase activity.[25] In addition to its function in apoptosis regulation, XIAP also performs other non-apoptotic biological functions. For example, XIAP participates in signal transduction and ubiquitination.[26] The current understanding of XIAP, particularly the function of its E3 ubiquitin ligase, remains limited. Therefore, we conducted an in-depth study on the potential mechanisms of XIAP in the apoptosis of Caki-1 cells, which are derived from a typical RCC cell line. We combined RNAi of XIAP with an iTRAQ-based quantitative proteomics approach to globally profile the function of XIAP in etoposide-induced apoptosis. Our iTRAQ results revealed that under apoptosis stimulation, changes in the XIAP protein level induce differential expression of proteins between the original Caki-1 cells and XIAP knockdown cells. The findings suggest that XIAP may be involved in regulating the expression of the identified differentially expressed proteins. We identified 1784 differentially expressed proteins between the two cell lines. We characterized proteins showing a ratio fold-change $\geq$1.3 or $\leq$0.77 as significantly altered proteins. GO enrichment analysis showed that the identified differentially expressed proteins are widely distributed in the cell and are involved in many aspects of cell biology. Collectively, these results indicate that XIAP is involved in numerous novel biological processes. Notably, we observed the highest number of differentially expressed proteins at 0.5 h after etoposide treatment. The number of differentially expressed proteins then drastically decreased at 12 h after etoposide treatment. Thus, we inferred that the functions of XIAP are mainly confined to a 3 h window after apoptosis induction and that initiation of the apoptotic signaling pathway is completed at 12 h after apoptosis induction.

Etoposide-induced DNA strand breaks are major triggers of DNA repair activation through histone proteins. DNA damage and repair are critical in a cell-free apoptosis system. Thus, we examined whether XIAP affects histones. XIAP silencing altered the expression of five histone variants (H1.4, H3.1, H3.2, H3.3, and H2AX) in etoposide-induced apoptosis. We found that except for H2AX, the remaining four proteins were highly expressed before the induction of apoptosis and that their ratios decreased after etoposide treatment. However, in Caki-1 cells, H2AX was downregulated at each time point. H1 histone variants directly affect the tightness of nucleosome packaging and the advanced structure of chromosomes by interacting with DNA.[27] The H3 family is composed of H3.1, H3.2, and H3.3 variants, which are highly conserved. H3.3 is a variant of histone proteins involved in transcriptional activation.[28] The caspase-3/CAD

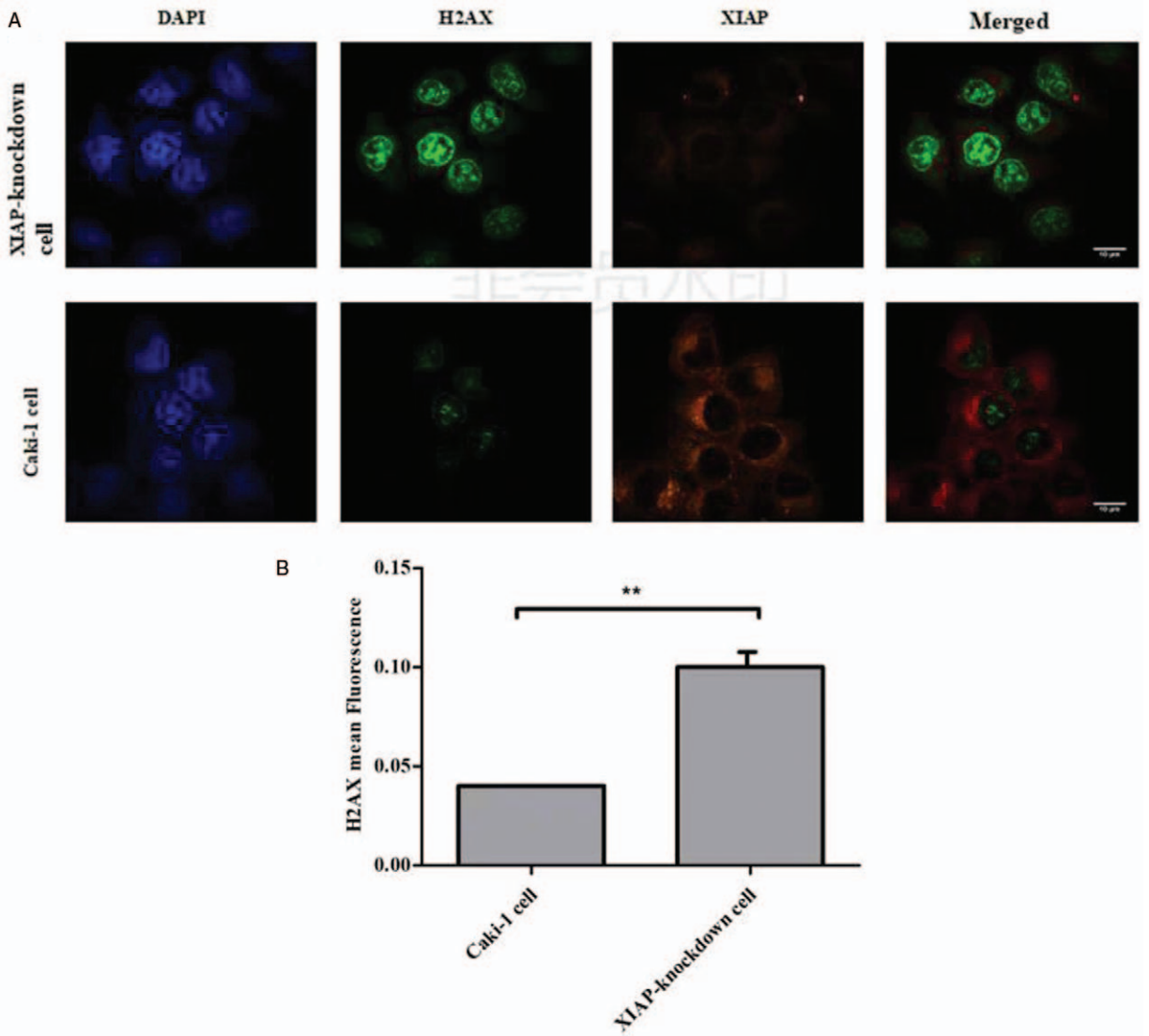

Figure 6: Sub-cellular distribution of XIAP and H2AX. (A) XIAP (red) and H2AX (green) expression in Caki-1 cells and XIAP knockdown cells was detected by immunofluorescence. Nuclear staining was performed with DAPI (blue). (B) Quantification of the H2AX staining is shown in the column bar graph, and the results are expressed as the mean fluorescence intensity. The data are shown as the mean ± SD. Experiments were repeated three times. $^{**}P < 0.01$ was considered statistically significant. DAPI: 4′,6-Diamino-2-phenylindole; XIAP: X-linked inhibitor of apoptosis.

(DFF40) pathway cannot induce DNA fragmentation in the absence of H2AX. Therefore, H1 and H3 may have minor roles in apoptosis induction, and their participation deserves further investigation.

Our Western blot analysis results revealed for the first time that XIAP knockdown induces upregulation of H2AX. Our Western blot analysis results validated our iTRAQ results. Therefore, our results collectively suggest that etoposide-induced DNA damage and DNA repair mechanisms likely depend on XIAP. Considering the E3 ubiquitin ligase activity of XIAP, we speculated that XIAP may decrease H2AX protein expression by directly ubiquitinating the H2AX protein via the ubiquitin proteasome pathway. However, under ordinary conditions, XIAP is distributed in the cytoplasm, and H2AX is distributed in the nucleus. Thus, to verify whether XIAP directly interacts with H2AX, we used confocal microscopy to detect the localization of XIAP-IF and H2AX-IF in the two cell lines. As shown in Figure 6, there was no colocalization of XIAP and H2AX. Therefore, XIAP may not directly regulate the protein level of H2AX through ubiquitination but instead affect H2AX through other signaling pathways in cells or regulate the transcriptional level of H2AX. It has been reported that the mitogen-activated protein kinase (MAPK) pathway regulates the protein and transcription level of histone H2AX protein.[29] Therefore, in follow-up studies, we will continue to explore whether XIAP can affect H2AX through the MAPK pathway in RCC. In addition, the effect of XIAP on apoptosis-related events in the nucleus can be clarified.

Conclusions

Our results indicate that XIAP can mediate apoptosis through multiple pathways, including DNA damage and DNA repair mechanisms, through downregulation of H2AX. The apoptotic pathway is activated if repair fails.

Although the regulation of H2AX expression in human RCC is not completely understood and demands further investigation, our data suggest that RCC cells with high XIAP expression are resistant to apoptosis and to reductions in H2AX. These findings provide a new direction for studying the radiation resistance of RCC and the potential function of XIAP.

Acknowledgement

The authors thank the Institute of Pathology of the Heinrich-Heine University German for providing the cell lines.

Funding

This work was supported by grants from the National Natural Science Foundation of China (No. 71432002) and the Beijing Municipal Commission of Education, Science and Technology plan projects (No. KM201310025017).

Conflicts of interest

None.

References

1. Armendariz BG, Masdeu Mdel M, Soriano E, Urena JM, Burgaya F. The diverse roles and multiple forms of focal adhesion kinase in brain. Eur J Neurosci 2014;40:3573–3590. doi: 10.1111/ejn.12737.
2. Mizutani Y, Nakanishi H, Li YN, Matsubara H, Yamamoto K, Sato N, *et al*. Overexpression of XIAP expression in renal cell carcinoma predicts a worse prognosis. Int J Oncol 2007;30:919–925. doi: 10.3892/ijo.30.4.919.
3. Yang WZ, Zhou H, Yan Y. XIAP underlies apoptosis resistance of renal cell carcinoma cells. Mol Med Rep 2018;17:125–130. doi: 10.3892/mmr.2017.7925.
4. Schimmer AD, Dalili S, Batey RA, Riedl SJ. Targeting XIAP for the treatment of malignancy. Cell Death Differ 2006;13:179–88. doi: 10.1038/sj.cdd.4401826.
5. Gyrd-Hansen M, Meier P. IAPs: from caspase inhibitors to modulators of NF-kappaB, inflammation and cancer. Nat Rev Cancer 2010;10:561–574. doi: 10.1038/nrc2889.
6. Liu J, Zhang D, Luo W, Yu J, Li J, Yu Y, *et al*. E3 ligase activity of XIAP RING domain is required for XIAP-mediated cancer cell migration, but not for its RhoGDI binding activity. PloS One 2012;7: e35682. doi: 10.1371/journal.pone.0035682.
7. Kaur S, Wang F, Venkatraman M, Arsura M. X-linked inhibitor of apoptosis (XIAP) inhibits c-Jun N-terminal kinase 1 (JNK1) activation by transforming growth factor beta1 (TGF-beta1) through ubiquitin-mediated proteosomal degradation of the TGF-beta1-activated kinase 1 (TAK1). J Biol Chem 2005;280:38599–38608. doi: 10.1074/jbc.M505671200.
8. Varghese J, Khandre NS, Sarin A. Caspase-3 activation is an early event and initiates apoptotic damage in a human leukemia cell line. ApoptosisV 8 2003;363–370. doi:10.1023/a:1024121017841.
9. Olayioye MA, Kaufmann H, Pakusch M, Vaux DL, Lindeman GJ, Visvader JE. XIAP-deficiency leads to delayed lobuloalveolar development in the mammary gland. Cell Death Differ 2005; 12:87–90. doi: 10.1038/sj.cdd.4401524.
10. Nowak D, Boehrer S, Brieger A, Kim SZ, Schaaf S, Hoelzer D, *et al*. Upon drug-induced apoptosis in lymphoma cells X-linked inhibitor of apoptosis (XIAP) translocates from the cytosol to the nucleus. Leuk Lymphoma 2004;45:1429–1436. doi: 10.1080/ 1042819042000198858.
11. Barker HE, Paget JT, Khan AA, Harrington KJ. The tumour microenvironment after radiotherapy: mechanisms of resistance and recurrence. Nat Rev Cancer 2015;15:409–425. doi: 10.1038/nrc3958.
12. Rogakou EP, Pilch DR, Orr AH, Ivanova VS, Bonner WM. DNA double-stranded breaks induce histone H2AX phosphorylation on serine 139. J Biol Chem 1998;273:5858–5868. doi: 10.1074/ jbc.273.10.5858.
13. Zhang J, He Y, Shen X, Jiang D, Wang Q, Liu Q, *et al*. Gamma-H2AX responds to DNA damage induced by long-term exposure to combined low-dose-rate neutron and gamma-ray radiation. Mut Res Genet Toxicol Environ Mutagen 2016;795:36–40. doi: 10.1016/j. mrgentox.2015.11.004.
14. Cook PJ, Ju BG, Telese F, Wang X, Glass CK, Rosenfeld MG. Tyrosine dephosphorylation of H2AX modulates apoptosis and survival decisions. Nature 2009;458:591–596. doi: 10.1038/na-ture07849.
15. Chen Y, Choong LY, Lin Q, Philp R, Wong CH, Ang BK, *et al*. Differential expression of novel tyrosine kinase substrates during breast cancer development. Mol Cell Proteomics 2007;6:2072–2087. doi: 10.1074/mcp.M700395-MCP200.
16. Smith NA, Byl JA, Mercer SL, Deweese JE, Osheroff N. Etoposide quinone is a covalent poison of human topoisomerase IIbeta. Biochemistry 2014;53:3229–3236. doi: 10.1021/bi500421q.
17. Chen C, Zhao SC, Yang WZ, Chen ZP, Yan Y. Potential biological process of X-linked inhibitor of apoptosis protein in renal cell carcinoma based upon differential protein expression analysis. Oncol Lett 2018;15:821–832. doi: 10.3892/ol.2017.7383.
18. Bilim V, Yuuki K, Itoi T, Muto A, Kato T, Nagaoka A, *et al*. Double inhibition of XIAP and Bcl-2 axis is beneficial for retrieving sensitivity of renal cell cancer to apoptosis. Br J Cancer 2008;98:941–949. doi: 10.1038/sj.bjc.6604268.
19. Hossain MA, Russell JC, O'Brien R, Laterra J. Neuronal pentraxin 1: a novel mediator of hypoxic-ischemic injury in neonatal brain. J Neurosci 2004;24:4187–4196. doi: 10.1523/JNEUROSCI.0347-04.2004.
20. Chong PK, Lee H, Zhou J, Liu SC, Loh MC, So JB, *et al*. Reduced plasma APOA1 level is associated with gastric tumor growth in MKN45 mouse xenograft model. J Proteomics 2010;73:1632–1640. doi: 10.1016/j.jprot.2010.04.005.
21. Roos WP, Krumm A. The multifaceted influence of histone deacetylases on DNA damage signalling and DNA repair. Nucleic Acids Res 2016;44:10017–10030. doi: 10.1093/nar/ gkw922.
22. Ljungberg B, Campbell SC, Choi HY, Jacqmin D, Lee JE, Weikert S, *et al*. The epidemiology of renal cell carcinoma. Eur Urol 2011;60:615–621. doi: 10.1016/j.eururo.2011.06.049.
23. Liston P, Roy N, Tamai K, Lefebvre C, Baird S, Cherton-Horvat G, *et al*. Suppression of apoptosis in mammalian cells by NAIP and a related family of IAP genes. Nature 1996;379:349–353. doi: 10.1038/379349a0.
24. Yan Y, Mahotka C, Heikaus S, Shibata T, Wethkamp N, Liebmann J, *et al*. Disturbed balance of expression between XIAP and Smac/ DIABLO during tumour progression in renal cell carcinomas. Br J Cancer 2004;91:1349–1357. doi: 10.1038/sj.bjc.6602127.
25. Yang Y, Fang S, Jensen JP, Weissman AM, Ashwell JD. Ubiquitin protein ligase activity of IAPs and their degradation in proteasomes in response to apoptotic stimuli. Science 2000;288:874–877. doi: 10.1126/science.288.5467.874.
26. Eckelman BP, Salvesen GS, Scott FL. Human inhibitor of apoptosis proteins: why XIAP is the black sheep of the family. EMBO Rep 2006;7:988–994. doi: 10.1038/sj.embor.7400795.
27. Furuhashi H, Takasaki T, Rechtsteiner A, Li T, Kimura H, Checchi PM, *et al*. Trans-generational epigenetic regulation of C. elegans primordial germ cells. Epigenetics Chromatin 2010;3:15. doi: 10.1186/1756-8935-3-15.
28. Ricketts MD, Frederick B, Hoff H, Tang Y, Schultz DC, Singh Rai T, *et al*. Ubinuclein-1 confers histone H3.3-specific-binding by the HIRA histone chaperone complex. Nat Commun 2015;6:7711. doi: 10.1038/ncomms8711.
29. Wu XP, Xiong M, Xu CS, Duan LN, Dong YQ, Luo Y, *et al*. Resveratrol induces apoptosis of human chronic myelogenous leukemia cells in vitro through p38 and JNK-regulated H2AX phosphorylation. Acta Pharmacol Sin 2015;36:353–361. doi: 10.1038/aps.2014.132.

How to cite this article: Liu TS, Chen C, Zhou B, Xia BW, Chen ZP, Yan Y. Isobaric tags for relative and absolute quantitation-based quantitative proteomic analysis of X-linked inhibitor of apoptosis and H2AX in etoposide-induced renal cell carcinoma apoptosis. Chin Med J 2019;132:2941–2949. doi: 10.1097/CM9.0000000000000553